Tree cover in the Taiga-Tundra Ecotone (TTE) : Landsat-based uncertainty and validation

K.J. Ranson, P. Montesano SSAI, C.S.R. Neigh, Biospheric Sciences, NASA GSFC
J. Sexton, S Channan, M. Feng, J. Townshend UMD, & M. Chopping Montclair State

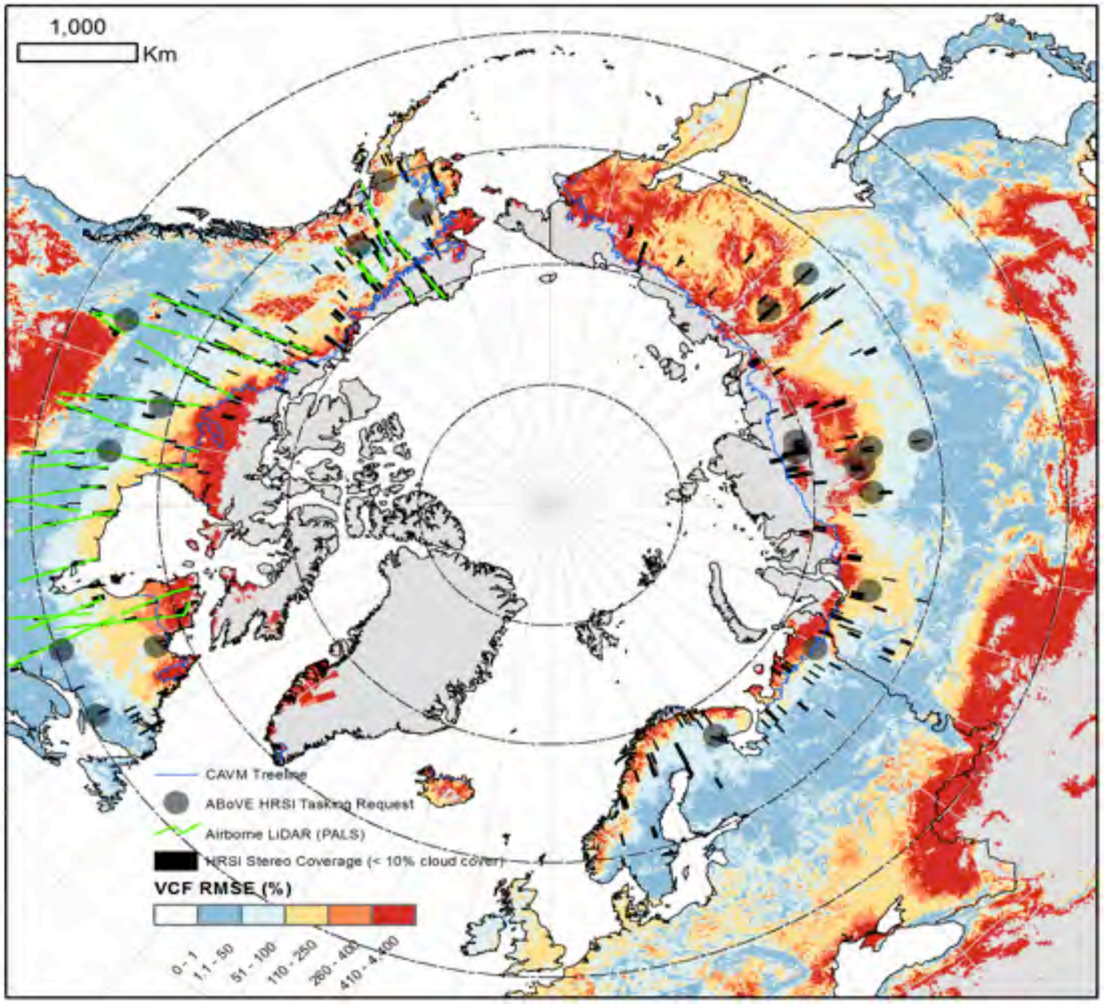

Figure 1

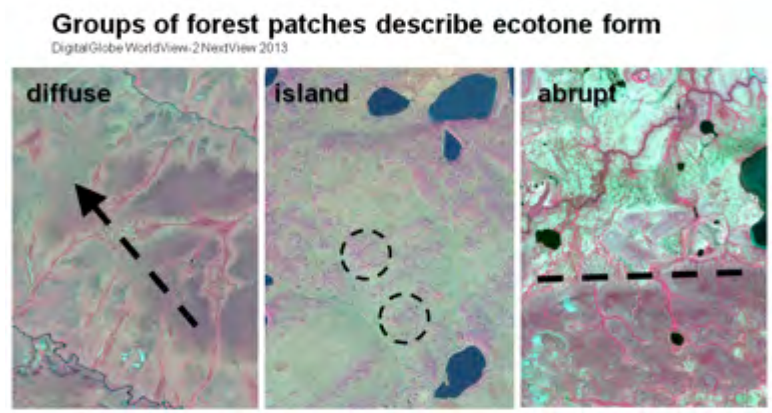

Figure 2

Climate change is expected to alter the tree line. A validated moderate resolution baseline is required to monitor change.

Name: K. Jon Ranson, Christopher S.R. Neigh, Biospheric Sciences, NASA GSFC ; Paul Montesano, SSAI
E-mail: kenneth.j.ranson@nasa.gov, christopher.s.neigh@nasa.gov; paul.m.montesano@nasa.gov
Phone: 301-614-6650

References:

2014 Montesano, P.M., Sun, G., Dubayah, R.O., Ranson, K.J. (2014). The Uncertainty of Plot-Scale Forest Height Estimates from Complementary Spaceborne Observations in the Taiga-Tundra Ecotone. *Remote Sensing*, 6, 10070-10088; doi:10.3390/rs61010070

2013 Sexton, J., X. Song, M. Feng, P. Noojipady, A. Anand, C. Huang*, et al., "Global, 30-m resolution continous fields of tree cover: Landsat-based rescaling of MODIS vegetation continous fields with lidar-based estimates of error," International Journal of Digital Earth, pp. 1-22.*

2013 Neigh, C.S.R. J. G. Masek, and J. Nickeson, "High-Resolution Satellite Data Open for Government Research," *EOS Transactions, vol. 94, pp. 121-123.*

2011 Ranson, K.J., Montesano, P.M., & Nelson, R. 2011. Object-based mapping of the circumpolar taiga-tundra ecotone with MODIS tree cover. *Remote Sensing of Environment,* 115(12):3670-3680.

2009 Montesano, P.M., Nelson, R., Sun, G., Margolis, H., Kerber, A., Ranson, K.J. 2009. MODIS tree cover validation for the circumpolar taiga-tundra transition zone, *Remote Sensing of Environment*, 113:2130-2141.

Technical Description of Images:

Figure 1. A preliminary 2005 estimate of percent tree cover uncertainty derived from the Landsat VCF tree cover product to improve our prior circumpolar arctic-boreal transition assessment. (Sexton et al. 2013)

Figure 2. WorldView-2 color-IR image examples of forest stands at the northern limit. Note that the so-called treeline can occur as an abrupt change from forest to tundra , a gradual decrease in tree cover (diffuse) or small fragmented stands (islands) at the taiga- tundra ecotone. High-resolution data with supercomputing are needed to document and understand overall TTE structure. We are using high-resolution panchromatic and stereo data in intensive study sites along the forest-tundra transition zone and characterizing the spatial patterns of the tree-tundra mosaic across the boundaries. This knowledge allows more accurate estimates of forest cover and biomass change across the larger TTE.

Scientific significance:
The spatial distribution and dynamics of tree cover is poorly understood across the full circumpolar domain. Refined estimates of tree cover in moderate and high resolutions will help inform analyses of tree cover change and tree structure vulnerability in the TTE.

Relevance for future science and relationship to Decadal Survey:
Forest carbon is a critical component of the carbon cycle, and is sensitive to climate change and disturbances. Forest structure observations from high-resolution commercial instruments are available at no direct cost through the National Geo-spatial Intelligence Agency (NGA) NextView license agreement with DigitalGlobe. Combining these data with moderate resolution forest cover estimates, airborne and field measurements could provide the necessary data products to accurately infer aboveground boreal forest carbon stocks. This technique is also valuable for estimating uncertainty of products from current and future potential decadal survey missions.

Nansen Ice Shelf GPS and tiltmeter field data to validate ice shelf flexure visco-elastic modeling.

Christine F. Dow, Cryospheric Sciences, NASA GSFC and NASA NPP
Ryan T. Walker, Cryospheric Sciences, NASA GSFC and University of Maryland

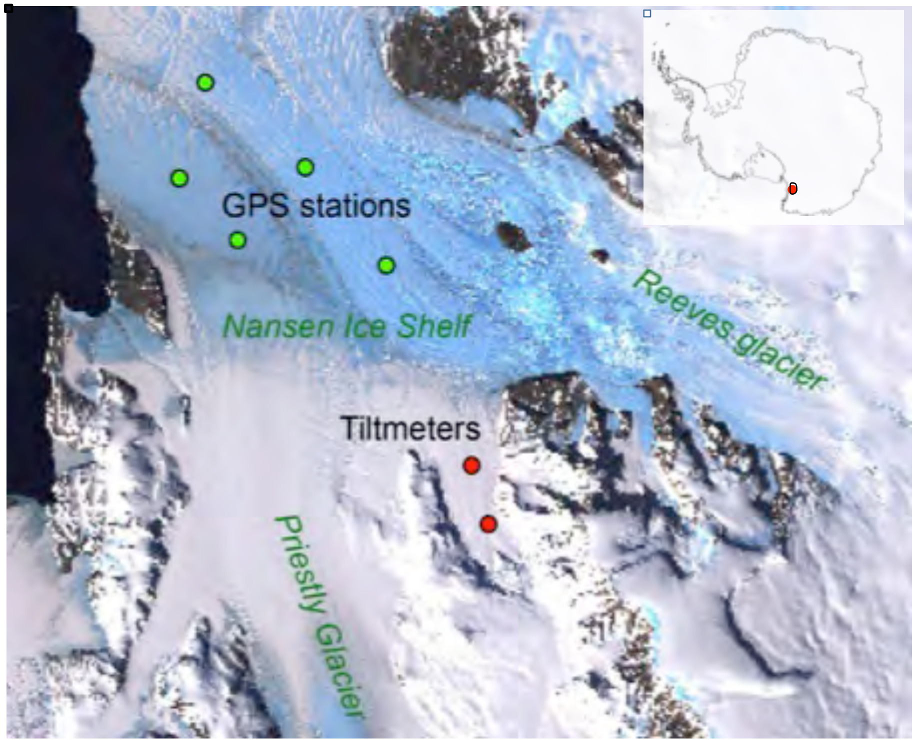

Figure 1

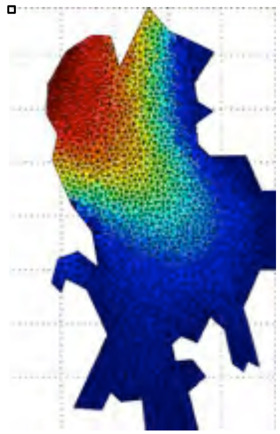

Figure 2

Figure 3

Figure 4

Fieldwork on the Nansen Ice Shelf in November and December 2015 involved successful installation of 5 GPS units and 2 tiltmeters to investigate ice flexure up to the ice grounding line.
Results will be used to validate models of visco-elastic ice shelf flexure and to estimate the impact of tidal variation on ice shelf and glacier dynamics.

Name: Christine F. Dow, Cryospheric Sciences, NASA GSFC, NASA NPP
E-mail: christine.f.dow@nasa.gov
Phone: 301-614-5299

References:
Additional collaborators – Dr. Won Sang Lee, Korean Polar Research Institute, Dr. Sridhar Anandakrishnan, Penn State University, Dr. Sophie Nowicki, NASA/GSFC

NASA earth observatory blog posts at: http://earthobservatory.nasa.gov/blogs/fromthefield/category/Nansen-ice-shelf-antarctica-2015/

Data Sources:
Landsat Image Mosaic of Antarctica (USGS); NASA IceBridge flight line from 19 November 2013 for ice surface and bed topography; Bindschadler, R., H. Choi, and ASAID Collaborators. 2011. *High-resolution Image-derived Grounding and Hydrostatic Lines for the Antarctic Ice Sheet.* Boulder, Colorado, USA: National Snow and Ice Data Center. http://dx.doi.org/10.7265/N56T0JK2.; Rignot, E., J. Mouginot, and B. Scheuchl. 2011. Antarctic Grounding Line Mapping from Differential Satellite Radar Interferometry, *Geophysical Research Letters*, 38, L10504, doi:10.1029/2011GL047109.

Technical Description of Figures:
Graphic 1: Landsat image mosaic with locations of GPS and tiltmeters installed on the Nansen Ice Shelf during November and December 2015.
Graphic 2: Preliminary model outputs showing magnitude of ice shelf maximum velocities using a visco-elastic ice flow model. Model outputs were used to determine installation positions for the field instrumentation.
Graphic 3: Photo shows NASA scientists with a GPS station installed on the Nansen Ice Shelf. Photo credit: Dr. Christine Dow.
Graphic 4: Photo shows NASA scientists and colleague from the Korean Polar Research Institute (KOPRI) installing one of the tiltmeters. Photo credit: Dr. Hyun-Jae Yoo.

Scientific significance, societal relevance, and relationships to future missions:
The ice shelves of the Antarctic are important for buttressing flow from surrounding glaciers (similar to corks in wine bottles, ice shelves influence the discharge rate of the inland ice sheet and resulting sea level rise). The impact of the flexure of these shelves due to tides and related horizontal motion on adjoining glacier dynamics is, however, not well understood. We are collaborating with scientists from the Korean Polar Research Institute to constrain the dynamic impact of ice shelf flexure using a combination of data collection and modeling approaches. During November and December 2015 we installed a suite of instruments including a) 5 dual-frequency geodetic GPS receivers on the body of the Nansen Ice Shelf and b) 2 high-precision tiltmeters placed near the grounding line where the glacier transitions from flowing on the bed to floating on ocean water. The data from these instruments will be used to constrain models of visco-elastic ice flexure that estimate transient perturbations of ice stress and velocity. These models provide important information on the stability of the ice grounding lines and subglacial conditions that directly impact ice flow. An accurate understanding of ice dynamics is crucial for interpretation of signals observed from NASA satellites, including changes in ice surface elevation that will be measured by ICESat2.

Challenges in remote sensing and simulation of irrigation

Sujay Kumar, Christa Peters-Lidard, Joseph Santanello, Grey Nearing, Mike Jasinski, Hydrological Sciences;
Rolf Reichle, Clara Draper, Randal Koster, GMAO, NASA GSFC

Figure 1

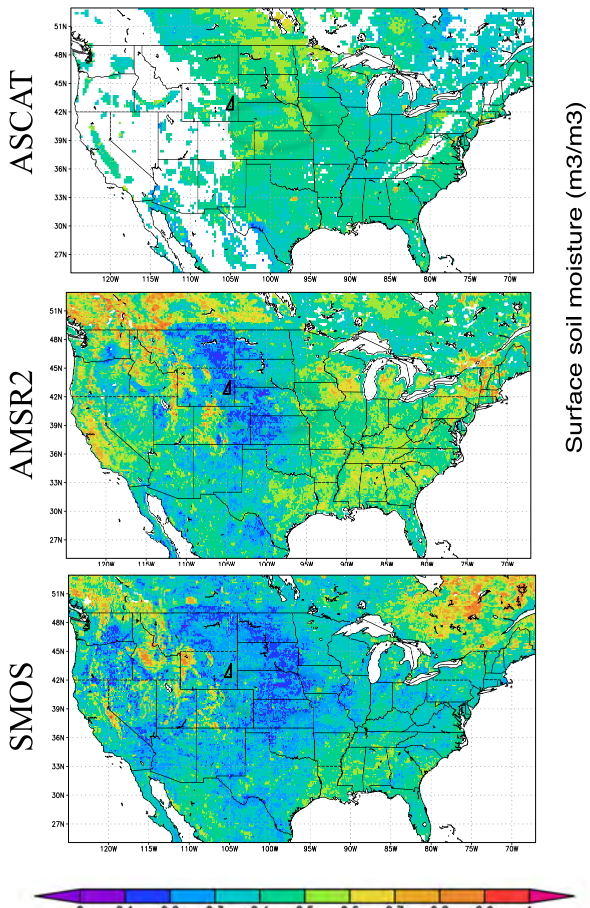

Unitless degree of difference between the remote sensing product and a model simulation that lacks irrigation

Figure 2

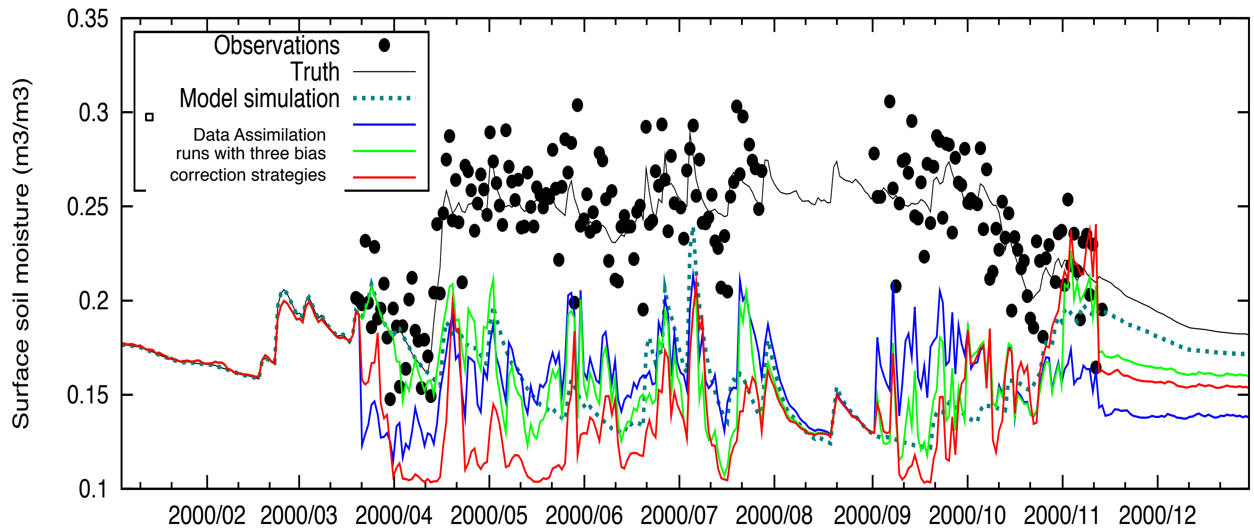

The skill of the passive microwave soil moisture retrievals in detecting features of large-scale seasonal irrigation was mixed, with ASCAT retrievals more effective than SMOS and AMSR2 products.

Current bias correction practices in land data assimilation systems do not account for unmodeled but real signals. In this experiment, signals of irrigation were mistakenly determined to be too wet and therefore not properly accounted for.

Name: Sujay V. Kumar, Hydrological Sciences, NASA GSFC
E-mail: sujay.v.kumar@nasa.gov
Phone: 301-286-8663

References:

Kumar, S.V., C.D. Peters-Lidard, J.A. Santanello, R.H. Reichle, C.S. Draper, R.D. Koster, G. Nearing, M.F. Jasinski, 2015: Evaluating the utility of satellite soil moisture retrievals over irrigated areas and the ability of land data assimilation methods to correct for unmodeled processes, *Hydrol. Earth Syst. Sci.*, 19, 4463-4478, doi:10.5194/hess-19-4483-2015.

Data Sources:
Soil moisture retrievals from the backscatter measurements acquired by Advanced Scatterometer (ASCAT), soil moisture retrievals from the Advanced Microwave Scanning Radiometer 2(AMSR2), soil moisture retrievals from the Soil Moisture Ocean Salinity (SMOS) mission. ASCAT retrievals are obtained through the Soil Moisture Operational Products System (SMOPS) of National Oceanic and Atmospheric Administration (NOAA)/National Environmental Satellite Data and Information Service (NESDIS). The level 3 AMSR2 data is obtained from the Japan Aerospace Exploration Agency (JAXA) and the level 2 swath-based SMOS products are obtained from the European Space Agency (ESA).

Technical Description of Images:

Figure 1. A quantitative comparison of the differences in soil moisture distributions between three remote sensing products (ASCAT, AMSR2, SMOS) and a model simulation that intentionally does not include formulations of irrigation. The maps show the Kolmogorov-Smirnov distance measure (D), which is an indication of the degree to which the soil moisture distributions from the two datasets differ. Values of D closer to zero indicates that the soil moisture distributions from the two datasets being compared are close to each other and larger D values indicate locations where the soil moisture distributions from the two integrations differ. The spatial patterns in these maps can be used as a first measure of whether a sensor captures the observational feature such as irrigation. For e.g., over a known hot-spot of irrigation such as the plains of Nebraska, values of D are close to zero in the SMOS and AMSR2 comparison, whereas ASCAT shows larger values. This is an indication that SMOS and AMSR2 are less skillful in detecting irrigation features compared to ASCAT.

Figure 2. A comparison of the use of different bias mitigation strategies in an idealized data assimilation (DA) integration when the significant source of biases are from an unmodeled process such as irrigation. Synthetic observations are generated from the synthetic 'Truth' and assimilated into the 'Model Simulation'.The three DA integrations represent the use of different bias correction strategies. Figure demonstrates that the DA integrations employing bias correction strategies do not incorporate the wet signal of irrigation. The bias correction methods are designed to treat the systematic differences between the model and observations (in this case from irrigation) as biases and exclude them in DA systems. As they make no distinction of the source of biases, the use of such practices lead to the exclusion of signals from unmodeled processes (such as irrigation).

Scientific significance:
This study demonstrates that the skill of the soil moisture retrievals must be improved in agricultural areas if they are to capture the artifacts of human engineered processes such as irrigation. The study also finds that new data assimilation and bias correction strategies are needed to preserve the observational information about unmodeled processes.

Relevance for future science and relationship to Decadal Survey:
Soil moisture measurements are critical for several societal applications including agricultural management. In order to realize their potential for such applications, it is important that soil moisture observations from missions such as Soil Moisture Active Passive (SMAP) include the impacts of both the natural variability as well as human engineering practices such as irrigation. Focused efforts must be made as part of both mission Cal/Val activities and retrieval algorithm development to improve the information content of soil moisture remote sensing measurements over agricultural areas. Similarly, data assimilation systems that ingest such measurements must adapt, so that unmodeled and subjective human engineered processes are accurately represented.

Urban Area Monitoring using MODIS Time Series Data

Sudipta Sarkar[1,2], Sadashiva Devadiga[1,2] and Edward Masuoka[1],
[1]Terrestrial Information Systems NASA GSFC, [2]SSAI

Figure 1

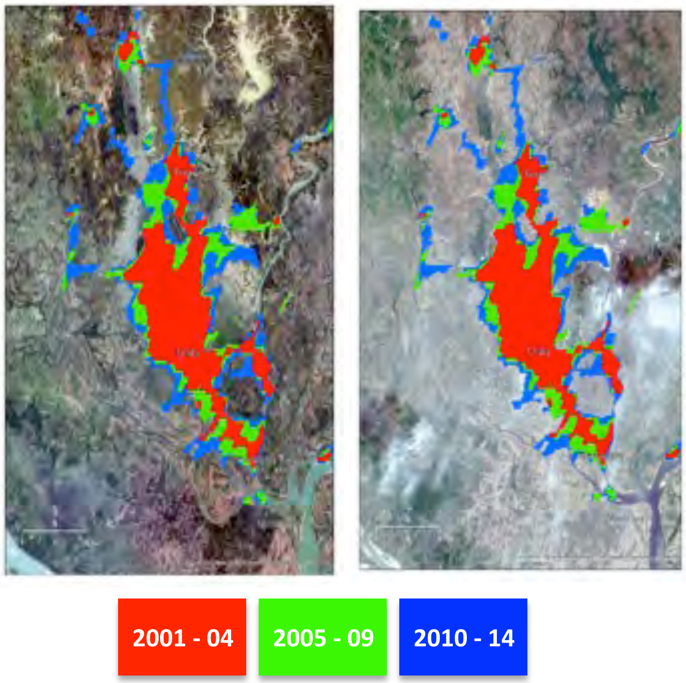

Figure 2

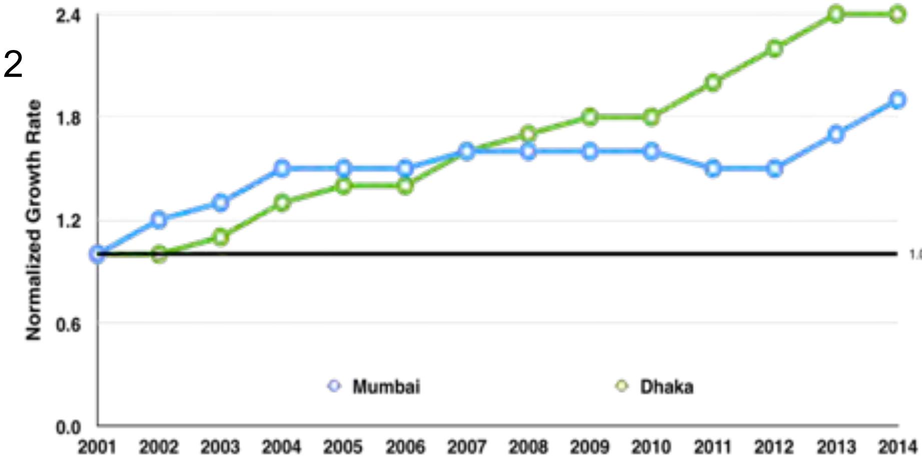

Figure 3

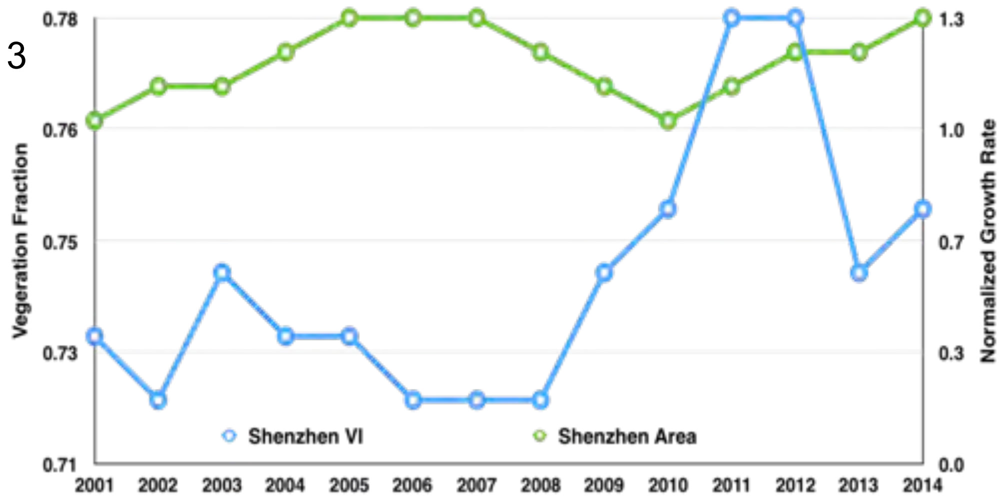

Urban growth in Dhaka after 2010 does not reflect economic slowdown like Mumbai. Detection of planned urban re-development in Shenzhen after 2011 shows an uptick in greening and apparent urban regression.

Name: Sudipta Sarkar, GSFC/SSAI, Code 619
E-mail: sudipta.sarkar@nasa.gov
Phone: (301) 614-6912

References

Sudipta Sarkar, Sadashiva Devadiga, Ed Masuoka “Urban area monitoring using MODIS time series data”. AGU Fall Meeting 2015, San Francisco.

Pu Hao, Richard Sliuzas, Stan Geertman “The development and redevelopment of urban villages in Shenzhen”. *Habitat International* 35(2011), 214-224.

Xu, H. "Modification of Normalized Difference Water Index (NDWI) to Enhance Open Water Features in Remotely Sensed Imagery." *International Journal of Remote Sensing* 27, No. 14 (2006): 3025-3033.

Zha, Y., J. Gao, and S. Ni. "Use of Normalized Difference Built-Up Index in Automatically Mapping Urban Areas from TM Imagery." *International Journal of Remote Sensing* 24, no. 3 (2003): 583-594.

Data Sources

MODIS Collection 5 Level 3 gridded products MOD13Q1 (250m 16-day Vegetation Indices), MOD11A2 (8-day Land Surface Temperature), MCD43A4 (16-day BRDF/Albedo), MCDLCHKM (500m multi-year Land Cover product), Collection 6 DEM (Digital Elevation Model)

Technical Description of Figures

Figure 1: Urban area mapped by our approach overlaid on the RGB composite image generated using the Landsat 7 data from day 2002336 (left) and Landsat 8 from day 2015076 (right) respectively. The urban map have been color coded to indicate the year in which urbanization was first detected.

Figure 2: Urban growth trend for major metropolitan cities in Asia like Mumbai showed almost static growth between 2007 and 2010 possibly because of the global recession. Cities like Dhaka in Bangladesh, on the other hand, do not show such coupling with global economy suggesting urban growth largely from residential development.

Figure 3: Some of the major cities like Shenzhen in China are undergoing urban redevelopment. A steady growth is seen for city of Shenzhen until 2005. Then a dip in the urban growth is seen with increased vegetation This relates to possible clearing up and redevelopment of the surrounding “urban villages” that came up during the initial stages of industrial growth around the region. Post 2011 we see another urban growth from the redevelopment of the urban village and the surrounding area.

Scientific Significance

This study uses time series of MODIS data to detect and monitor urban area expansion. Several annual metrics are computed from the gridded data products such as Vegetation Indices, Land Surface Temperature and Albedo, at 250 meter resolution and are segmented using a vector angle mapping classifier to detect urban area. This was applied to delineate the urban area for cities in Asia, showing maximum growth in the last 15 years. The results were verified using high resolution Landsat data.

Growing urban sprawl has significant impact on the global climate caused by the urban heat island effects and anthropogenic aerosol emissions. This is even more significant in the recent years because of the rapid urbanization that is happening in some of the fast developing nations across the globe. It also puts more pressure on global food supply as it encroaches on cultivable lands.

Near-real-time VIIRS Imagery and Fires

Carol Davidson, Diane Davies, Greg Ederer, Neal Devine, Gary Fu, Cynthia Hamilton,
Maki Jackson, Anhquan Nguyen, Jeff Schmaltz, Gang Ye,
Terrestrial Information Systems, NASA GSFC, Science Systems & Applications/Global Science & Technology

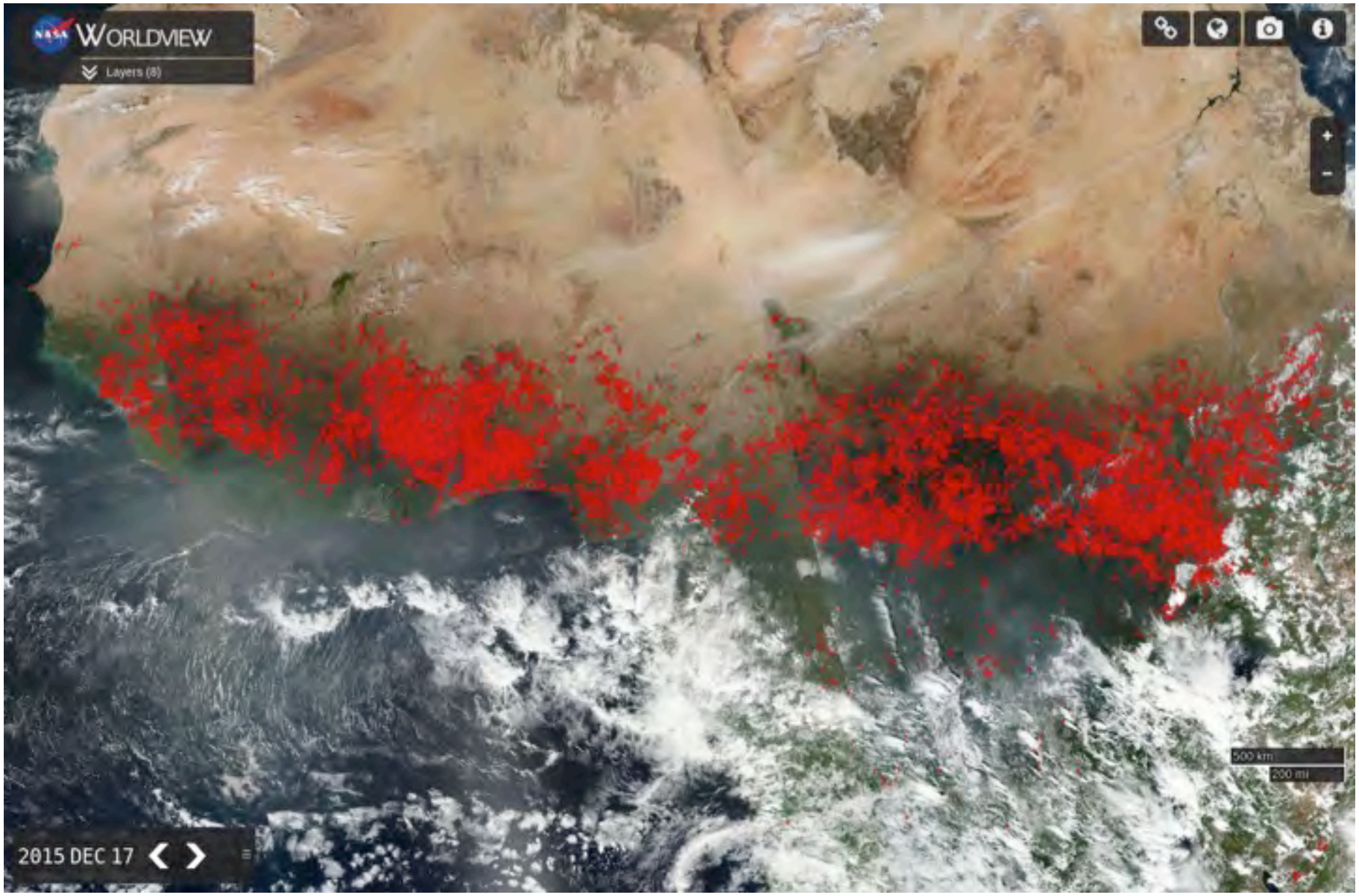

Full-globe imagery and I-band (375m resolution) fire detections from the VIIRS instrument aboard the Suomi NPP are now available at full resolution in NASA's Worldview imagery browser and Global Imagery Browse Services (GIBS)

Name: Jeff Schmaltz, Terrestrial Information Systems, NASA GSFC / SSAI
E-mail: Jeff.Schmaltz@nasa.gov
Phone: (301) 614-5135

References:

Schmaltz, J., C. Alarcon, R. Boller, M. Cechini, C. De Cesare, A. De Luca, J. Hall, T. Huang, J. King, L. Plesea, N. Pressley, J. Roberts, J. Rodriguez, C. Thompson. 2015. “Newer, bigger, older” with NASA GIBS. Poster. American Geophysical Union Fall Meeting, December 14-18, 2015, San Francisco, CA.

Data Sources: The VIIRS corrected reflectance was developed by Code 619, the VIIRS I-band (375m resolution) fire detection was developed by the VIIRS Active Fire Team at the University of Maryland, and the VIIRS corrected reflectance and fire data and imagery are generated by Code 619 in the LANCE near-real-time system.

Technical Description of Figures:

Figure 1: Screen capture from the NASA Worldview image browser showing VIIRS Corrected Reflectance imagery and VIIRS I-band (375m resolution) fire detections from 17 December 2015. VIIRS imagery has complete coverage at the equator, with no inter-orbit gaps. The I-band fire detections provide much more detail than was previously available for global daily coverage. The perennial dust source of the Bodélé Depression can also be seen in this image. (URL for this view: http://go.nasa.gov/1OCLZm8)

Scientific significance:

The availability of these new near-real-time imagery layers in NASA’s Global Imagery Browse Services (GIBS) and the Worldview browser will make it easier and quicker for science and application users to find NASA VIIRS data that they need to do their work.